

# Dual function for the adaptor MIST in IFN- $\gamma$ production by NK and CD4<sup>+</sup>NKT cells regulated by the Src kinase Fgr

Hiroki Sasanuma, Akiko Tatsuno, Shinya Hidano, Keiko Ohshima, Yumi Matsuzaki, Katsuhiko Hayashi, Clifford A. Lowell, Daisuke Kitamura, and Ryo Goitsuka

**Natural killer (NK) cells and NKT cells play critical early roles in host defense. Here we show that MIST, an adaptor protein belonging to the SLP-76 family, functions negatively in NK cells but positively in CD4<sup>+</sup>NKT cells. NK-cell receptor-mediated IFN- $\gamma$  production was enhanced in NK cells, whereas TCR- or NK-cell receptor-mediated cytokine production was reduced in CD4<sup>+</sup>NKT cells from MIST-**

**deficient mice. These opposite effects of MIST paralleled the exclusive expression of the Src family kinase, Fgr, in NK cells between the 2 cell populations. We further demonstrated that interaction of MIST with Fgr, mediated by the C-terminal proline-rich region of MIST and the SH3 domain of Fgr, was required for the suppression of NK-cell receptor-induced IFN- $\gamma$  production. This functional interde-**

**pendence of signaling molecules demonstrates a new mechanism by which adaptor proteins can act as molecular switches to control diverse responses in different cell populations. (Blood. 2006;107:3647-3655)**

© 2006 by The American Society of Hematology

## Introduction

Natural killer (NK) and NKT cells act as major effector-cell populations at the front line of immune defense, eliminating pathogens and tumor cells without prior sensitization and producing cytokines that recruit and educate cells mediating a subsequent adaptive immune response.<sup>1,2</sup> Unlike T and B lymphocytes, which recognize aberrant cells using T-cell receptors (TCRs) and B-cell receptors (BCRs) whose genes undergo rearrangements to generate diversity, NK cells use a diverse array of nonrearranging receptors each specific for different ligands.<sup>3</sup> NKT cells express both the receptors characteristic of NK cells and a TCR composed of an invariant V $\alpha$ 14-J $\alpha$ 281 chain and a restricted V $\beta$  repertoire.<sup>4</sup> By using this restricted TCR, NKT cells, particularly a CD4<sup>+</sup> subset of NKT cells, are able to recognize glycolipid antigens in the context of CD1d,<sup>5</sup> a major histocompatibility complex (MHC) class I-like molecule, at the earliest stage of the immune response and secrete large amounts of cytokines.<sup>2</sup>

NK cells are activated to become cytotoxic and produce IFN- $\gamma$ . Activation is dependent on receptors, such as NKR-P1C (also called as NK1.1), CD16, and Ly49H, and their associated signaling chains, such as DAP12<sup>6</sup> and the Fc receptor  $\gamma$  chain (FcR $\gamma$ ),<sup>7</sup> which carry immunoreceptor tyrosine-based activation motifs (ITAMs) in their cytoplasmic tails. ITAM-bearing receptors, in common with TCRs and BCRs, are thought to transduce signals via sequential activation of protein tyrosine kinases (PTKs), phosphatases, and other enzymes. Another receptor that mediates NK-cell activation, NKG2D, can signal not only through ITAM-containing DAP12 but also through DAP10,<sup>8,9</sup> which carries a YINM motif that activates phosphatidylinositol 3 (PI3) kinase.<sup>8</sup>

Adaptor proteins play a key regulatory role in linking receptor-proximal signals to downstream effector molecules.<sup>10</sup> Adaptor molecules lack enzymatic activities but possess multiple structural modules for protein-protein interactions, which allow them to function as scaffold molecules for PTKs, effectors, and other adaptors and so facilitate signal transduction. Among these adaptor proteins, SLP-76 adaptor family members have been demonstrated to play key roles in the specific cell lineages that express them. SLP-76 has been demonstrated to be essential for pre-TCR signaling during T-cell development,<sup>11,12</sup> collagen receptor signaling in platelets,<sup>13</sup> and high-affinity IgE receptor signaling in mast cells.<sup>14</sup> Furthermore, a deficiency in BASH (also known as BLNK and SLP-65), a B-lineage cell-specific member of SLP-76 family, causes impaired B-cell development due to defective pre-BCR and BCR signaling.<sup>15-18</sup>

MIST (also named Clnk) is the third member of the SLP-76 adaptor protein family<sup>19,20</sup> and is expressed in cytokine-activated hematopoietic cells including mast cells and NK cells. In common with other family members, MIST contains 3 protein interaction domains. Its aminoterminal carries tyrosine residues, which are phosphorylated by Src family PTKs and also by Syk.<sup>21</sup> The central region contains 2 proline-rich sequences: the N-terminal one interacts with an SH3 domain of PLC $\gamma$  and the C-terminal one with that of Grb2.<sup>21</sup> The C-terminal SH2 domain of MIST acts as a binding site for ADAP (previously known as SLAP-130/Fyb)<sup>22</sup> as well as a hematopoietic serine/threonine kinase, HPK-1.<sup>23</sup> MIST interacts with similar but not identical signaling molecules to SLP-76 or BLNK and has been demonstrated to restore defective

From the Division of Molecular Biology, Research Institute for Biological Sciences, Tokyo University of Science, Noda, Japan; Department of Physiology, Keio University School of Medicine, Tokyo, Japan; and Department of Laboratory Medicine, University of California, San Francisco.

Submitted October 17, 2005; accepted December 27, 2005. Prepublished online as *Blood* First Edition Paper, January 26, 2006; DOI 10.1182/blood-2005-10-4102.

Supported by grants from the Japanese Ministry of Education, Culture, Sports, Science and Technology (MEXT) (R.G., D.K.) and by the Japan

Science and Technology Agency (R.G.).

**Reprints:** Ryo Goitsuka, Division of Molecular Biology, Research Institute for Biological Sciences, Tokyo University of Science, 2669 Yamazaki, Noda, Chiba 278-0022, Japan; e-mail: ryogoi@rs.noda.tus.ac.jp.

The publication costs of this article were defrayed in part by page charge payment. Therefore, and solely to indicate this fact, this article is hereby marked "advertisement" in accordance with 18 U.S.C. section 1734.

© 2006 by The American Society of Hematology

TCR signaling in an SLP-76-deficient Jurkat T-cell line and defective BCR-signaling in a BLNK-deficient B-cell line, when the raft-associated linker for activation of T cells (LAT) is coexpressed.<sup>21,23</sup> Contrary to these *in vitro* data that suggest MIST is a positive regulator of immunoreceptor signaling, Utting et al have recently reported that the natural cytotoxicity of Clnk-deficient NK cells is modestly enhanced.<sup>24</sup> However, the detailed functional role of Clnk/MIST in NK-cell activation remains to be elucidated.

Here we describe the generation and characterization of MIST-deficient mice and demonstrate that MIST is not simply a positive regulator of immunoreceptor signaling but has dual functions depending on the cell context: it acts as a negative regulator in NK cells and as a positive regulator in CD4<sup>+</sup>NKT cells. We further demonstrate that this functional dichotomy is determined by the differential expression of a Src family PTK, Fgr, in the 2 cell types.

## Materials and methods

### Mice

MIST-deficient mice were generated as follows. The homologous regions of the final vector consisted of a 5.75-kb genomic fragment immediately upstream of the MIST translation initiation codon and a 0.85-kb DNA fragment immediately downstream of the second exon. The EGFP neomycin-resistant gene cassette, which replaced 50 bp of the second exon encoding the first 6 amino acids with the 5' part of second intron, was constructed using an EGFP cDNA including an SV40 polyadenylation signal sequence (pEGFP-C1; Clontech, Palo Alto, CA) and a *loxP*-flanked neomycin gene derived from pGK neo. All the fragments were assembled into the pKSTKLoxPNeo targeting vector containing the HSV thymidine kinase gene (HSV-TK). The resultant MIST-targeting construct was electroporated into E14 ES cells, and drug-resistant colonies were screened for homologous recombination. Targeted clones were injected into C57BL/6 blastocysts and produced progeny having germ-line transmission of the mutated allele. Fertilized eggs from female C57BL/6 mice crossed with male *MIST*<sup>+/*neo*</sup> mice were transiently injected with pCre-pac plasmid to delete the neomycin selection cassette from the mutated allele to generate *MIST*<sup>+/*Δneo*</sup> mice. *MIST*<sup>+/*neo*</sup> mice backcrossed 8 times to a BALB/c background and *MIST*<sup>+/*Δneo*</sup> mice backcrossed 8 to 10 times to a C57BL/6 background were used to obtain homozygous mice. Fgr-deficient mice on the C57BL/6 background were generated as previously described.<sup>25</sup>

### Flow cytometry

Single-cell suspensions from the indicated organ were stained with a combination of FITC-, PE-, and biotin-conjugated antibodies, followed by streptavidin-PerCP-Cy5.5 (BD Biosciences, San Jose, CA). The conjugated and unconjugated antibodies specific to the following antigens were purchased from BD Biosciences and eBioscience (San Diego, CA): CD16, TCRαβ, NK1.1, CD3ε, B220, DX-5, c-kit, CD4, CD8α, CD11b, CD11c, CD1d, Ly49A, Ly49D, Ly49C/I, Ly49G2, and CD94. Data were collected on a FACSort flow cytometer (Becton Dickinson, San Jose, CA) and analyzed using CELLQuest software (Becton Dickinson).

### NK and CD4<sup>+</sup>NKT-cell preparation

NK cells were enriched by depleting fresh spleen-cell suspensions of B cells, CD8<sup>+</sup> cells, and CD4<sup>+</sup> T cells using anti-CD19, -CD8, and -CD4 antibody-coated microbeads on a magnetic-activated cell separator (MACS) (Miltenyi Biotec, Auburn, CA). Anti-CD19 and -CD8 antibody-coated beads were used for CD4<sup>+</sup>NKT-cell enrichment. Thereafter, NK-cell- or CD4<sup>+</sup>NKT-cell-enriched suspensions were stained with anti-NK1.1 and anti-TCRαβ antibodies or with anti-NK1.1 and anti-CD4 antibodies. NK1.1<sup>+</sup>TCRαβ<sup>-</sup>NK cells and NK1.1<sup>+</sup> CD4<sup>+</sup>NKT cells were sorted to more than 95% purity using a FACSvantage (Becton Dickinson) or MoFlo (Cytomation, Fort Collins, CO). Purified cells were cultured in RPMI 1640 medium supplemented with 10% FCS and antibiotics (Gibco, Grand Island,

NY) in the presence of recombinant mouse IL-2 (2000 U/mL) for 5 to 7 days. The purity of IL-2-expanded NK1.1<sup>+</sup>TCRαβ<sup>-</sup>NK cells and NK1.1<sup>+</sup>CD4<sup>+</sup>NKT cells was more than 98% on the day of assay.

### Killing assay

Standard 4-hour <sup>51</sup>Cr-release assays were performed as described previously.<sup>7</sup> Briefly, 1 × 10<sup>6</sup> target cells were incubated with 100 μCi (3.7 MBq) Na<sub>2</sub><sup>51</sup>CrO<sub>4</sub> (Amersham, Arlington Heights, IL) for 1 hour and were washed extensively. Fluorescence-activated cell sorter (FACS)-sorted NK cells cultured for 5 to 7 days in the presence of IL-2 were added to the target cells (4 × 10<sup>3</sup> cells per well) in triplicate wells of U-bottomed microtiter plates in a final volume of 200 μL. Target cells used were YAC-1, EL-4, and EL-4 precoated with an anti-Thy1.2 antibody.

### Cytokine production

To detect intracellular IFN-γ, sorted spleen NK or CD4<sup>+</sup>NKT cells expanded with IL-2 were incubated in the presence of 2 μM monensin (Sigma-Aldrich, St Louis, MO) for 6 hours in microtiter plates precoated with anti-NK1.1 (50 μg/mL), anti-Ly46D (100 μg/mL), anti-CD3 (50 μg/mL), or in the presence of PMA (50 ng/mL) plus ionomycin (1 μM). To prevent Fc receptor-dependent activation, cells were pretreated with a soluble 2.4G2 antibody for 30 minutes on ice unless used for anti-CD16 stimulation experiments. Cells were fixed in 4% paraformaldehyde, permeabilized in a solution containing 0.5% Triton X-100, and then stained with anti-IFN-γ-PE (XMG1.2; BD Biosciences). NK cells or NKT cells were also cultured in flat-bottomed microtiter plates in the presence of IL-2 and stimulated with immobilized antibodies or with IL-12 (10 ng/mL). Target cells were also cocultured with NK cells in U-bottomed microtiter plates at the ratio of 1:1. After 24 hours of culture, the cell-free supernatants were collected, and the level of IFN-γ and IL-4 was measured using specific ELISA kits (BioSource, Camarillo, CA). Spleen cells (5 × 10<sup>5</sup>/200 μL) were also stimulated with 50 ng/mL α-galactosylceramide (α-GalCer; Kirin Brewery, Tokyo, Japan) or vehicle as a control for 72 hours. Culture supernatants were harvested to measure cytokine levels. For *in vivo* stimulation, mice were injected intraperitoneally with α-GalCer (2 μg/200 μL) or vehicle. Serum was collected from treated mice at the indicated time points.

### Measurement of intracellular calcium

IL-2-expanded NK cells were incubated with the calcium-sensitive dye Indo 1-AM (Molecular Probes, Eugene, OR) in the presence of F-127 and 0.2% FCS at 37°C for 30 minutes. Cells were washed twice and stained with anti-NK1.1 antibody for 30 minutes on ice. Cells were washed and stimulated with the anti-mouse IgG F(ab')<sub>2</sub> antibody at 37°C to cross-link precoated anti-NK1.1 antibody in phenol red-free RPMI 1640 medium containing 0.1% FCS. Cells were also stimulated with 1 μg/mL ionomycin. Calcium mobilization was analyzed in BD-LSR (BD Biosciences). Values were plotted as ratio of fluorescence at FL4 (Ca<sup>2+</sup>-free indo-1) and FL5 (Ca<sup>2+</sup>-bound indo-1).

### Biochemical analysis

IL-2-expanded NK cells were starved for 4 hours in the absence of IL-2 and incubated on ice for 30 minutes with 10 μg/mL anti-NK1.1 antibody and then with the anti-mouse IgG F(ab')<sub>2</sub> antibody (20 μg/mL) at 37°C for the indicated time. Cell lysates were immunoprecipitated and blotted with the indicated antibodies. Blots were scanned and analyzed with Molecular Analyst software (Bio-Rad, Hercules, CA). COS-7 cell transfection, immunoprecipitation, and immunoblotting experiments were carried out as previously described.<sup>20</sup> Antibodies against Fgr, PLCγ2, ERK2, and p38 (Santa Cruz Biotechnology, Santa Cruz, CA), phospho-PLCγ2 (Cell Signaling Technology, Beverly, MA), phospho-ERK and phospho-p38 (Promega, Madison, WI), GFP (Molecular Probes), and MIST were used as described previously.<sup>20</sup>

### Retrovirus transduction

The cDNAs of mouse MIST, Fgr, and their mutants<sup>21,26</sup> were inserted into a pMX-IRES-GFP bicistronic retrovirus vector.<sup>27</sup> Each of the resulting

plasmids was transfected into a packaging cell line, PLAT-E, using FuGENE6 (Roche, Milan, Italy), and after 24 hours of incubation the culture supernatants were harvested and concentrated as viral stocks. FACS-sorted NK and CD4<sup>+</sup>NKT cells were cultured in IL-2 for 48 hours and then transfected with retrovirus in the presence of 0.5 μg/mL Polybrene (Sigma-Aldrich) for 48 hours. Cells were cultured for an additional 2 days in the presence of IL-2 and then stained for intracellular IFN-γ. The GFP fluorescence emitted by the retroviruses was at least 10 times brighter than the knock-in EGFP fluorescence, by flow cytometry analysis, and did not interfere with the distinction of cDNA transfected from untransfected cells. These recombinant retroviruses were also used to infect avian B-cell line DT40 cells stably expressing the mouse ecotropic retrovirus receptor<sup>28</sup> DT40-ETR (provided by Dr T. Mizuno, Yamaguchi University, Japan) to verify the level of protein expression with bicistronically expressed GFP.

### Reverse transcriptase–polymerase chain reaction (RT-PCR) analyses

Total RNA was isolated using TRIZOL reagent (Gibco BRL, Grand Island, NY) and converted into single-stranded cDNA using SuperScriptII reverse transcriptase with oligo-(dT) primer (Invitrogen, Carlsbad, CA). The resultant cDNAs were subjected to PCR for MIST, Fgr, or β-actin mRNA using the following specific primers: 5'-CTTACAGAGTGTCCAG-GATGCGACCGTGG-3' and 5'-GAGGGGTGGTACTTCTTGGGGAGAG-TGATAGC-3' for MIST, 5'-TGGTGGGGGAATACCTAATATGCAAGAT-CG-3' and 5'-TGCCAGTCAGGCTATGTCTGGTCTCCAGG-3' for Fgr, and 5'-TACAATGAGCTGCGTGTGGC-3' and 5'-TAGCTC TTCTCCAGGGA-GG-3' for β-actin.

### Experimental metastasis model

B16 melanoma cells ( $2 \times 10^5$  cells) or Colon-26 carcinoma cells ( $2.5 \times 10^4$  cells) were injected intravenously into syngeneic wild-type and MIST-deficient mice (4 mice per group) on C57BL/6 or BALB/c backgrounds. Mice were killed 14 days later, and metastatic nodules on the lung surface were counted and photographed using a Leica MZAPO stereomicroscope (50 mm aperture and  $1 \times$  objective lens; Leica, Deerfield, IL) with a digital camera (Olympus, Tokyo, Japan). To deplete NK cells, mice were injected intraperitoneally with anti- $\alpha$ -asialo GM1 antibody (150 μg per mouse; Wako Chemicals, Tokyo, Japan) 2 days before inoculation of B16 cells ( $2 \times 10^4$  cells) and also 3 and 8 days after the inoculation. The effectiveness of the depletion was confirmed by the absence of NK1.1<sup>+</sup>CD3<sup>-</sup> cells in spleens from treated mice. The number of NKT cells was not affected by the anti- $\alpha$ -asialo GM1 antibody treatment.

### Statistical analysis

Comparisons were analyzed for statistical significance by the Student *t* test using Microsoft Excel software (Microsoft, Redmond, CA), with *P* below .05 being considered significant.

## Results

### MIST is dispensable for NK- and NKT-cell development

We inactivated the *MIST* gene in mice by gene targeting in which the second *MIST* exon encoding the first methionine was replaced with an EGFP cDNA and a *loxP*-flanked neomycin resistance gene (*neo<sup>R</sup>*) cassette (Figure 1A-B). The *neo<sup>R</sup>* was removed from the mutant alleles of the heterozygous mice (*MIST<sup>+/neo</sup>*) through Cre-mediated recombination to generate *MIST<sup>+/ $\Delta$ neo</sup>* mice (Figure 1B, right panel). Expression of any forms of MIST RNA and protein was undetectable in IL-3–induced bone marrow–derived mast cells (BMMCs) (Figure 1C-D) and in IL-2–expanded spleen NK and NKT cells from both *MIST<sup>neo/neo</sup>* and *MIST $\Delta$ neo/ $\Delta$ neo* mice (Figure 1D and data not shown). We therefore concluded that these mice carry a null mutation in the *MIST* gene.

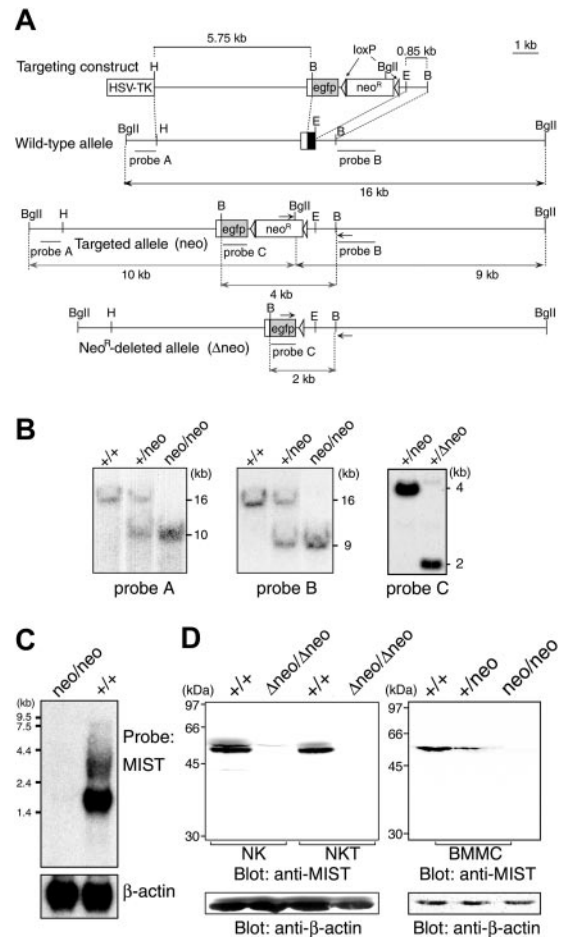


**Figure 1. Generation of MIST-deficient mice.** (A) Genetic modification of the *MIST* locus. Configuration of the wild-type *MIST* locus, the targeting vector, the *MIST* locus (*MIST<sup>neo</sup>*) after homologous recombination of the targeting vector, and *MIST* locus (*MIST $\Delta$ neo*) following Cre recombinase–mediated deletion of the *loxP*-flanked neomycin-resistant cassette. *MIST* exon 2 (white rectangle for the 5′-noncoding region and black rectangle for the coding region containing the initiation ATG), lengths of diagnostic restriction, probes A, B, and C (underlined), and PCR primers (horizontal arrows) used for genotyping are shown. B indicates *Bam*HI; BgII, *Bgl*II; E, *Eco*RI; H, *Hind*III. (B) Southern blot analysis of genomic DNA from wild-type and MIST-deficient mice. When hybridized with probe A (left panel) or probe B (middle panel), DNA from wild-type mice shows the expected 16-kb band, while DNA from *MIST<sup>+/neo</sup>* and *MIST<sup>neo/neo</sup>* mice contains the 10-kb band for probe A or 9-kb band for probe B, indicative of homologous integration into the *MIST* locus. Hybridization of *Eco*RI-digested DNA with probe C confirms deletion of the *loxP*-flanked *neo* gene from the mutant allele in *MIST<sup>+/Δneo</sup>* mice (2-kb band in right panel). (C) Northern blot analysis of MIST mRNA expression. Total RNA obtained from bone marrow–derived mast cells of wild-type and MIST-deficient mice was hybridized with a full-length mouse *MIST* cDNA probe. Stripping and reprobing of the filter with a β-actin probe shows equal RNA loading. (D) Western blot analysis to confirm loss of MIST expression in null homozygous littermates. Whole-cell lysates from spleen NK and NKT cells (left panel) and mast cells (right panel) were blotted with an anti-MIST antibody. Stripping and reprobing of the filter with an anti-β-actin antibody shows equal protein loading.

Development of NK cells as well as NKT cells in the liver and spleen was normal in MIST-deficient mice (Figure 2A). Furthermore, the proportion of NK cells that express the MHC class I–specific inhibitory receptors (Ly49A, Ly49C/I, Ly49G2, and CD94) as well as the activating receptor (Ly49D, NKR-P1C, and CD16) was normal in MIST-deficient NK cells, and their level of expression was also comparable to wild-type NK cells (Figure 2A-B). These data indicate that MIST is dispensable for NK- and NKT-cell development. We also used *MIST<sup>+/Δneo</sup>* mice bearing a knock-in EGFP gene under the transcriptional control of the endogenous *MIST* promoter to examine the expression of *MIST* in spleen cells. In nonstimulated spleen cells, only marginal EGFP

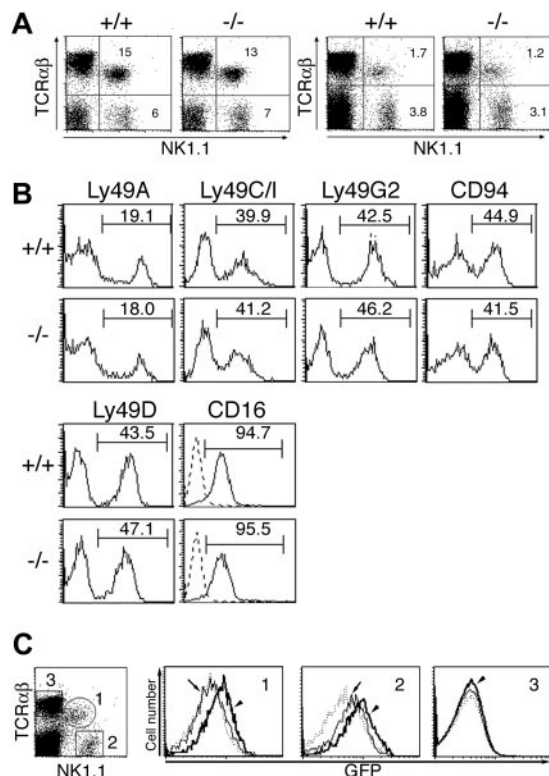


**Figure 2. MIST is dispensable for development of NK and NKT cells.** (A) Cells isolated from liver (left) and spleen (right) of 4- to 6-week-old MIST-deficient mice (-/-) and their littermates (+/+) were stained with the indicated antibodies and analyzed by flow cytometry. The percentages of gated cells are shown. Data are representative of 4 independent experiments. (B) Expression of inhibitory receptors as well as activating receptors on NK1.1<sup>+</sup>TCRαβ<sup>-</sup> NK cells from MIST-deficient mice. Histograms indicate expression of various inhibitory receptors (Ly receptors and CD94) and other activating receptors (NK1.1 and CD16) on NK cells in MIST-deficient (-/-) and wild-type NK cells (+/+). The gate used to calculate the percentage of cells expressing each receptor is shown by a horizontal line above each histogram. All histograms are representative of analyses from at least 3 mice of each genotype. (C) Flow cytometric analysis of knock-in EGFP fluorescence in spleen cells left unstimulated (arrows) or stimulated with α-GalCer (arrowheads) for 12 hours. FACS plot is shown for each set of markers, because there were no significant differences in phenotype between wild-type and MIST<sup>+/-Δneo</sup> mice. For each of the gated populations indicated, histograms for EGFP fluorescence were generated. Wild-type histograms (dotted lines) were overlaid with mutant histograms (solid lines).

fluorescence was detectable in NK cells, and the NKT and conventional T cells were negative (Figure 2C). However, EGFP fluorescence was rapidly induced in NKT cells in response to α-GalCer, a specific ligand for the invariant TCR expressed on these cells<sup>29</sup> (Figure 2C, arrowhead in histogram 1). EGFP fluorescence was also enhanced in NK cells by this treatment (Figure 2C, arrowhead in histogram 2), probably the result of induction by cytokines released from activated NKT cells. No EGFP enhancement was detectable in conventional T cells (Figure 2C, histogram 3), indicating that MIST expression in NK and NKT cells is up-regulated by activating signals.

#### MIST negatively regulates NK-cell receptor-mediated activation of NK cells

Because MIST is highly expressed in NK and NKT cells, we examined the impact of MIST deficiency on the function of these cells in vitro. IL-2-activated spleen NK cells from MIST-deficient mice killed NK-sensitive YAC-1 cells more efficiently than those from wild-type mice (Figure 3A, left panel). As for YAC-1 cells, the killing of antibody-coated EL-4 cells by IL-2-stimulated

MIST-deficient NK cells was enhanced compared with that by wild-type NK cells (Figure 3A, middle and right panels).

IFN-γ production is an important effector function of NK cells as well as NKT cells. MIST-deficient NK cells stimulated with anti-NK1.1 or Ly49D antibodies for 6 hours produced a higher frequency of IFN-γ-positive cells than did wild-type cells, as evaluated by intracellular IFN-γ staining (Figure 3B). The IFN-γ level in supernatants from MIST-deficient NK cells stimulated with antibodies against NKR-P1C or with YAC-1 target cells was also significantly higher than those from wild-type NK cells (Figure 3C). MIST-deficient and wild-type NK cells produced similar levels of IFN-γ in response to the nonspecific stimuli, PMA plus ionomycin or IL-12 (Figure 3 B-C), indicating no general abnormality in MIST-deficient NK cells. These findings indicate that MIST normally acts as a negative regulator of signal transduction from NK-cell-activating receptors to induce IFN-γ production.

#### Attenuated NKT-cell activation in MIST-deficient mice

We next examined the impact of MIST deficiency on NKT-cell activation mediated by an NK-cell receptor or by TCR. In contrast to NK cells, MIST-deficient CD4<sup>+</sup>NK1.1<sup>+</sup>NKT cells showed a reduced rather than enhanced NKR-P1C-induced IFN-γ production compared with wild-type NKT cells (Figure 3D, left panel). Furthermore, the level of IFN-γ produced by MIST-deficient NKT cells after CD3 cross-linking was significantly lower than that produced by wild-type NKT cells (Figure 3D, right panel). We further examined TCR-mediated activation of NKT cells using α-GalCer.<sup>29</sup> High levels of IL-4 and IFN-γ were detectable in supernatants of α-GalCer-stimulated spleen cells from wild-type mice, whereas the level of cytokines produced by MIST-deficient spleen cells was significantly lower (Figure 3E). Furthermore, the administration of α-GalCer in vivo resulted in the rapid elevation of serum IL-4 at 2 hours and IFN-γ at 16 hours in wild-type littermates, whereas MIST-deficient mice displayed significantly lower serum IL-4 and IFN-γ levels (Figure 3F). Thus, the observation suggests impairment in the TCR-mediated activation of MIST-deficient NKT cells. These findings demonstrate that MIST functions as a negative regulator of receptor signaling in NK cells but as a positive regulator of both TCR and NK-cell receptor signaling in CD4<sup>+</sup>NKT cells.

#### The C-terminal proline-rich domain of MIST is involved in the suppression of NK-cell receptor-mediated IFN-γ production

To dissect the functional domains of MIST involved in negative regulation of NK-cell receptor-mediated signaling, we next used retrovirus-mediated reconstitution of MIST-deficient cells with wild-type or mutant forms of MIST (Figure 4A). The retrovirus-mediated expression of these MIST mutants was confirmed by using pMX-IRES-GFP retrovirus vectors encoding various MIST mutants to infect DT40 cells stably expressing the mouse ecotropic retrovirus receptor DT40-ETR. All the mutants were expressed at a similar level to wild-type MIST (Figure 4A). Compared with cells infected with a control virus, wild-type MIST attenuated the enhanced IFN-γ production to a level comparable to normal NK cells (Figure 4B). Expression of MIST mutants containing 6 tyrosine-to-phenylalanine substitutions (YF) or a nonfunctional SH2 domain (R335K) also reversed the enhancement in NK-cell activation seen in MIST-deficient cells. However, a mutant lacking the C-terminal proline-rich domain (ΔPR2) failed to reverse the enhanced IFN-γ production, and a mutant lacking the N-terminal

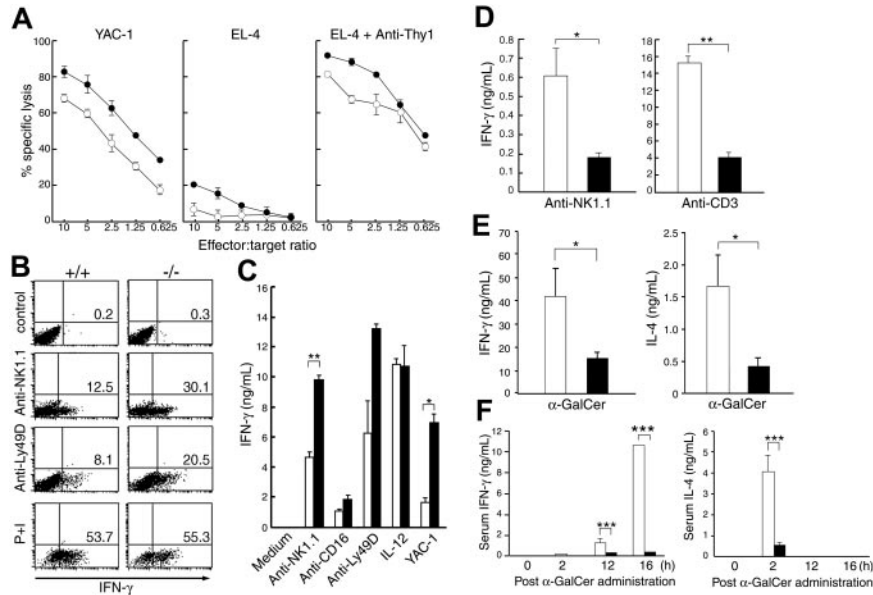


**Figure 3. Oposing functions of MIST in NK- and NKT-cell activation.** (A) IL-2–expanded spleen NK cells from wild-type (○) and MIST-deficient mice (●) were assayed for natural cytotoxic activities against YAC-1 and for antibody-mediated cytotoxicity against EL-4 cells either nontreated or pretreated with an anti-Thy1.2 antibody. Data are shown as the mean values and standard deviation (bars) of 1 representative from 3 independent experiments. (B) IL-2–expanded wild-type (+/+) and MIST-deficient (-/-) NK cells were stimulated with anti-NK1.1, anti-Ly49D antibodies, or PMA plus ionomycin (P+I) and assayed for intracellular IFN- $\gamma$ . The percentages of IFN- $\gamma$ -positive cells are indicated in the top right quadrants. (C) IL-2–expanded wild-type (□) and MIST-deficient (■) NK cells were cultured for 24 hours with the indicated antibodies, target cells, or with IL-12, and the amounts of IFN- $\gamma$  were measured. Data are the mean and standard deviation of at least 4 independent experiments. (D) IL-2–expanded NKT cells from MIST-deficient mice (■) and wild-type littermates (□) were stimulated with the indicated antibodies, and the amounts of IFN- $\gamma$  in the supernatants were measured. (E) Freshly isolated spleen cells ( $5 \times 10^5/200 \mu\text{L}$ ) from MIST-deficient mice (■) and wild-type littermates (□) were cultured with 50 ng/mL  $\alpha$ -GalCer for 72 hours. Culture supernatants were harvested to measure IFN- $\gamma$  and IL-4 levels as described in “Materials and methods.” (F) Serum IFN- $\gamma$  and IL-4 levels in MIST-deficient mice (■) and wild-type littermates (□) at different times after the administration of  $\alpha$ -GalCer. Data are the mean and standard deviation of at least 3 independent experiments. The statistical analysis was performed using the Student *t* test. (\**P* < .05; \*\**P* < .01; \*\*\**P* < .001).

proline-rich domain ( $\Delta$ PR1) only slightly reversed the MIST-deficient phenotype (Figure 4B). In contrast to NK cells, the  $\Delta$ PR2 mutant restored NKR-P1C–induced IFN- $\gamma$  production in MIST-deficient NKT cells to a level comparable to that by wild-type MIST (Figure 4C). These results indicate that the signaling intermediates associated with the C-terminal proline-rich domain are essential for MIST-mediated negative regulation of NKR-P1C–mediated NK-cell activation but not necessary for its positive function in NKT cells.

**Interaction of MIST with a Src family kinase Fgr is required for MIST-mediated suppression of NK-cell receptor–mediated IFN- $\gamma$  production**

To identify a binding partner of MIST, we performed yeast 2-hybrid screening and have identified Fgr, a hematopoietic Src family PTK (our unpublished data, July 2002). Fgr mRNA was detectable in NK cells but not in CD4<sup>+</sup>NK1.1<sup>+</sup> NKT cells (Figure 5A), and Fgr protein coprecipitated with MIST from NK cells

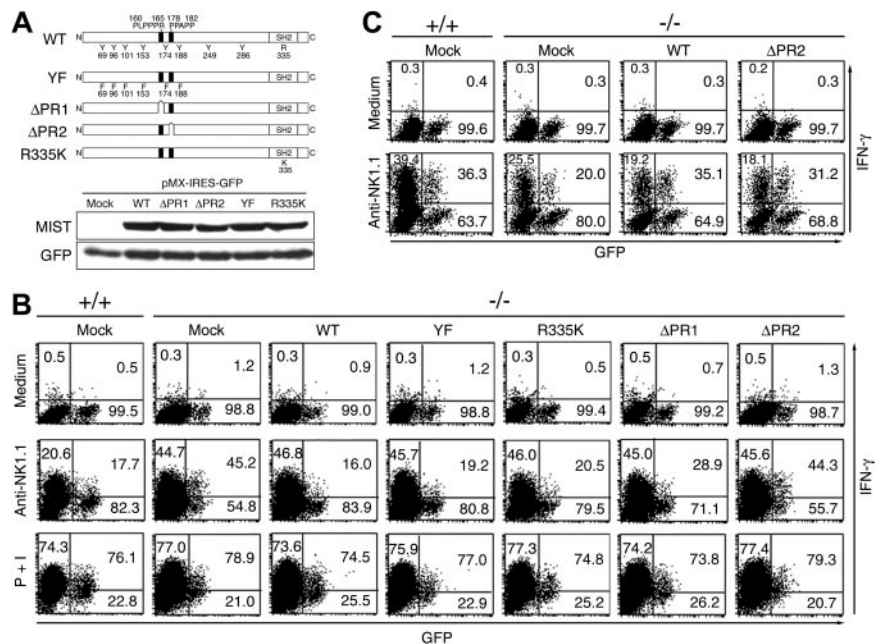


**Figure 4. The C-terminal proline-rich domain of MIST is required for its negative function in NK1.1-induced IFN- $\gamma$  production by NK cells.** (A) Schematic representation of MIST mutants and their protein expression. DT40-ETR cells were infected with pMX-IRES-GFP retrovirus vectors encoding wild-type (WT) and MIST mutants. Cell lysates from GFP-positive cells were immunoblotted with anti-MIST and anti-GFP antibodies. (B-C) IFN- $\gamma$  production by MIST-deficient NK cells (B) and CD4<sup>+</sup>NKT cells (C) reconstituted with various MIST mutants. Results for mock-infected wild-type (+/+) NK cells are shown in the first panels for comparison. The numbers are the percentages of IFN- $\gamma$ -producing and nonproducing cells in the GFP-positive population. The percentages of IFN- $\gamma$ -producing cells in the noninfected cell population are also shown in the top left quadrant. Representative data from 2 independent experiments are shown.

(Figure 5B). Fgr was associated with the  $\Delta$ PR1 mutant but not with the  $\Delta$ PR2 mutant. Furthermore, the association of MIST with Fgr was abolished by mutation of the SH3 domain of Fgr (W102A/W103A), indicating that Fgr is indeed associated with the C-terminal proline-rich region of MIST via its SH3 domain (Figure 5C). To examine the functional significance of the interaction of MIST with Fgr in NKR-P1C-mediated IFN- $\gamma$  production, we ectopically expressed Fgr in MIST-heterozygous and MIST-deficient CD4<sup>+</sup>NK1.1<sup>+</sup> NKT cells, which lack endogenous Fgr expression (Figure 5A). The NKR-P1C-induced IFN- $\gamma$  production by MIST-sufficient NKT cells was profoundly suppressed by the ectopic expression of Fgr, whereas expression of Fgr in MIST-deficient NKT cells had no effect (Figure 5D, upper middle panels), indicating that MIST is required for Fgr-mediated suppression of NK-cell receptor-induced activation. CD3-mediated IFN- $\gamma$  production was also consistently reduced by the selective introduction of Fgr in MIST-sufficient cells, although the effect was weaker than that observed after anti-NK1.1 stimulation (Figure 5D, lower middle panels).

### The SH3 domain but not kinase domain of Fgr is required for its negative function in NK-cell receptor-mediated IFN- $\gamma$ production

To further confirm the inhibitory role of MIST-Fgr interaction in NK-cell activation, we examined IFN- $\gamma$  production by NK cells from Fgr-deficient mice.<sup>25</sup> As observed in MIST-deficient NK cells, Fgr deficiency enhanced NKR-P1C-induced IFN- $\gamma$  production by NK cells (Figure 5E-G). This enhancement was reversed to the level comparable to that produced by wild-type NK cells by retrovirus-mediated introduction of wild-type Fgr as well as the kinase-inactive mutant form (KD) but not of the nonfunctional SH3 mutant (Figure 5G). Because Fgr associates with MIST via its SH3 domain (Figure 5C), these results indicate that Fgr is indeed involved in the negative regulation of the NK-cell activating receptor signaling and also suggest that this inhibitory function of Fgr is exerted by its SH3 domain-mediated interaction with the C-terminal proline-rich region of MIST but not by its kinase activity. In addition, the level of IFN- $\gamma$  produced upon  $\alpha$ -GalCer stimulation by Fgr-deficient spleen cells was comparable with that

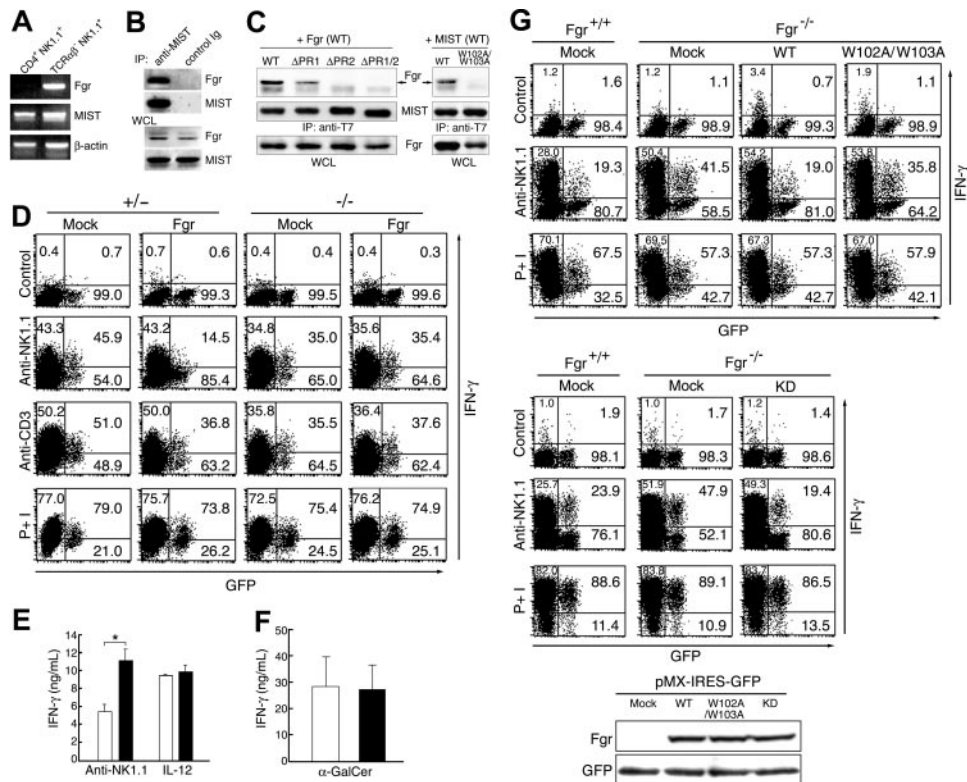


**Figure 5. Interaction of MIST with Fgr is essential for the attenuation of NK-cell receptor-mediated activation.** (A) Expression of Fgr mRNA in NK but not NKT cells. The cDNAs were synthesized from total RNA obtained from IL-2-expanded FACS-sorted spleen NK (NK1.1<sup>+</sup>TCR $\alpha\beta$ <sup>-</sup>) and NKT (NK1.1<sup>+</sup>CD4<sup>+</sup>) cells. PCR was carried out for Fgr, MIST, and  $\beta$ -actin mRNA using the specific primer pairs described in "Materials and methods." (B) Constitutive association of MIST with Fgr in NK cells. Cell lysates from wild-type NK cells were immunoprecipitated (IP) with anti-MIST or control antibody and immunoblotted with anti-Fgr or anti-MIST antibody. Whole-cell lysates (WCL) were also blotted with the same antibodies. (C) Association of Fgr with the C-terminal proline-rich region of MIST. COS-7 cells were transfected with expression plasmids encoding Fgr (left) in combination with that encoding T7 epitope-tagged wild-type (WT) or mutant forms of MIST lacking either single proline-rich domains ( $\Delta$ PR1 and  $\Delta$ PR2) or both ( $\Delta$ PR1/2) or transfected with MIST plasmid (right) in combination with Fgr (WT) or the nonfunctional SH3 domain mutant (W102A/W103A). Cell lysates were immunoprecipitated with anti-T7 antibody and then blotted with anti-Fgr or anti-MIST antibody. WCLs were also blotted with anti-Fgr antibody, which showed equal expression levels of Fgr protein. (D) Ectopic expression of Fgr attenuated NK1.1-mediated IFN- $\gamma$  production in MIST-sufficient but not in MIST-deficient NKT cells. IL-2-expanded NKT (NK1.1<sup>+</sup>CD4<sup>+</sup>) cells were transduced with a bicistronic retrovirus expressing Fgr with EGFP, stimulated either with anti-NK1.1, anti-CD3, or PMA plus ionomycin (P+I), and analyzed for intracellular IFN- $\gamma$ . The numbers represent percentages of IFN- $\gamma$ -producing and nonproducing cells in GFP-positive populations. The percentages of IFN- $\gamma$ -producing cells in the noninfected cell population are also shown in the top left quadrant. Representative data from 3 independent experiments are shown. (E) IFN- $\gamma$  release from wild-type ( $\square$ ) and Fgr-deficient NK cells ( $\blacksquare$ ) stimulated with the anti-NK1.1 antibody or IL-12. \* $P < .05$ . (F)  $\alpha$ -GalCer-induced IFN- $\gamma$  release from freshly isolated spleen cells from Fgr-deficient ( $\blacksquare$ ) and wild-type mice ( $\square$ ). (G) IFN- $\gamma$  production by Fgr-deficient NK cells reconstituted with wild-type Fgr, its nonfunctional SH3 domain, or kinase-inactive (KD) mutants. The percentages of IFN- $\gamma$ -producing and nonproducing cells in the GFP-positive- and -negative populations are shown as in Figure 6D. Data are representative of 2 independent experiments. The retrovirus-mediated expression of wild-type and mutant forms of Fgr protein was confirmed by Western blotting as described in Figure 4A.

produced by wild-type cells (Figure 5F), functionally supporting our observation that Fgr is absent in CD4<sup>+</sup>NKT cells. Taken together, these results demonstrate that collaboration of MIST and Fgr is required for their inhibitory functions in NK-cell receptor-mediated IFN- $\gamma$  production.

#### NKR-P1C–induced activation of PLC $\gamma$ 2 signaling is enhanced in MIST-deficient NK cells

To gain an insight into how MIST negatively regulates NK-cell receptor–mediated IFN- $\gamma$  production, we examined the biochemical events in NK cells triggered by NKR-P1C engagement. The increase in intracellular Ca<sup>2+</sup> level upon NKR-P1C engagement was enhanced and prolonged in MIST-deficient NK cells, compared with that in wild-type cells (Figure 6A). Consistent with this, NKR-P1C–induced phosphorylation of PLC $\gamma$ 2 was enhanced 5-fold, and the level was sustained in MIST-deficient NK cells (Figure 6B). We next examined MAP kinase activation because ERK and p38 have been shown to be implicated in the control of IFN- $\gamma$  production by NK cells.<sup>30</sup> Enhanced and sustained activation of ERK (1.5-fold and 4-fold for ERK1 and ERK2, respectively) and p38 MAP kinase (2-fold) was observed in NKR-P1C–stimulated MIST-deficient NK cells (Figure 6B). These data indicate that the NK-cell receptor–mediated activation of PLC $\gamma$ 2 and its downstream signaling pathways is enhanced in the NK cells devoid of MIST. Because PLC $\gamma$ 2 is essential for NKR-P1C–induced IFN- $\gamma$  production,<sup>31</sup> hyperactivation of PLC $\gamma$ 2 appears to be mainly responsible for the enhanced IFN- $\gamma$  production by MIST-deficient NK cells.

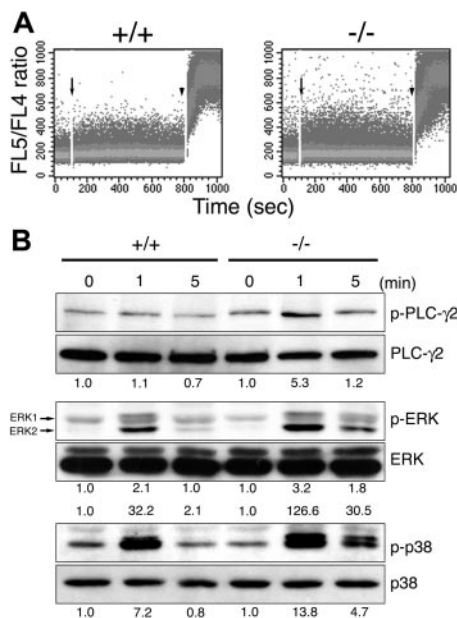


**Figure 6. Enhanced NKR-P1C–induced signaling in MIST-deficient NK cells.** (A) NKR-P1C–induced intracellular calcium flux in MIST-deficient NK cells. Wild-type (+/+) and MIST-deficient (-/-) NK cells loaded with Indo 1-AM were stimulated with anti-NK1.1 antibody. The ratio of fluorescence detected in FL5-FL4 was monitored by flow cytometry. Acquisition was interrupted once to add cross-linking goat F(ab')<sub>2</sub> antibody (arrows) and again to add 1  $\mu$ g/mL iomycin (arrowheads). (B) Enhanced phosphorylation of PLC $\gamma$ 2, ERK, and p38 MAP kinases in MIST-deficient NK cells upon NKR-P1C stimulation. Cell lysates from wild-type (+/+) and MIST-deficient (-/-) NK cells stimulated with anti-NK1.1 antibody were immunoblotted with the indicated antibodies. Figures give induction levels over zero time points, determined by densitometry after normalizing for loading.

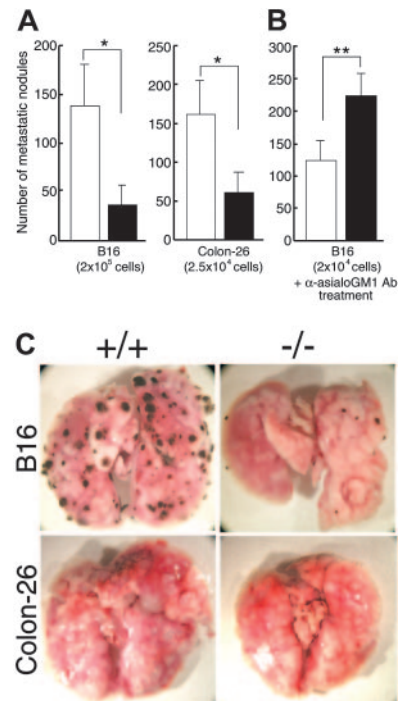


**Figure 7. MIST deficiency protects mice from lung metastases.** (A) B16 melanoma cells and Colon-26 carcinoma cells were injected intravenously into syngeneic wild-type (□) and MIST-deficient mice (■) on the C57BL/6 and BALB/c background (4 mice per group), respectively, and metastatic nodules were counted 14 days later. (B) Number of metastatic nodules formed by B16 melanoma cells in the lungs of wild-type and MIST-deficient mice treated with anti-asialo GM1 antibody to deplete NK cells, as described in “Materials and methods.” Statistical analysis was performed using the Student *t* test (\**P* < .01; \*\**P* < .005). (C) Representative photographs of metastatic nodules in the lung are shown.

#### Tumor-resistant phenotype of MIST-deficient mice

Finally, we examined the effects of MIST deficiency in vivo tumor metastasis models to determine whether the enhanced IFN- $\gamma$  production and cytotoxicity shown by MIST-deficient NK cells in vitro would have a biologic consequence in vivo. The Colon-26 adenocarcinoma cell line derived from BALB/c mice and the B16 melanoma cell line from C57BL/6 mice formed abundant metastases in the lung when injected intravenously into syngeneic wild-type mice (Figure 7). However, both the number and size of metastatic tumor nodules were significantly lower in the lungs of MIST-deficient mice (Figure 7). To confirm the cell population responsible for this enhanced tumor immunity, MIST-deficient mice were treated with anti-asialo GM1 antibody to selectively eliminate NK cells. In line with the previous report indicating that NK cells play the main role in the protection of lung metastasis of B16 melanoma cells,<sup>32,33</sup> the NK-cell depletion caused an increase in the number of metastatic nodules in both wild-type and MIST-deficient mice. We thus challenged the NK-cell–depleted mice with 10-fold fewer B16 melanoma cells ( $2 \times 10^4$  cells per mouse). As shown in Figure 7B, the MIST-deficient mice showed a higher rate of metastasis than wild-type mice in the absence of NK cells, indicating that NK cells are mainly responsible for the enhanced tumor resistance in MIST-deficient mice and also suggesting a defect of other cells, perhaps CD4<sup>+</sup>NKT cells, in the tumor resistance in MIST-deficient mice.

## Discussion

We demonstrate here that the adaptor molecule MIST negatively regulates NK-cell receptor–induced IFN- $\gamma$  production in NK cells that express the Src family PTK, Fgr, but acts positively in CD4<sup>+</sup>NKT cells, in which Fgr is not normally expressed.

Information regarding signal transduction from NK-cell activation receptors is now emerging, particularly concerning the roles of non-ITAM– and ITAM-bearing receptors in regulating the 2 important effector functions, natural cytotoxicity and IFN- $\gamma$  production.<sup>34</sup> Experiments using mice deficient for different signaling proteins have revealed that the signaling pathways from NK-cell receptors are not completely analogous to those used by BCRs and TCRs. For example, although Syk and ZAP-70 PTKs are essential components for BCR and TCR signal transduction,<sup>35,36</sup> NK cells lacking both Syk and ZAP-70 are still able to activate cytotoxicity and IFN- $\gamma$  production through a non-ITAM–bearing NK-cell receptor-activated pathway but not through ITAM-bearing receptors.<sup>37</sup> In the presence of pharmacologic inhibitors of Src-PTK– and PI3-kinase–mediated pathways, almost all the NK-cell receptor–mediated activation was abolished in Syk/ZAP-70–deficient NK cells, suggesting that natural cytotoxicity and IFN- $\gamma$  production by NK cells are regulated by synergistic and redundant signaling pathways involving Src-PTKs, Syk/ZAP-70, and/or PI3-kinase.<sup>34</sup> Based on our data that MIST-deficient NK cells showed enhanced receptor-induced calcium responses as well as PLC $\gamma$ 2 phosphorylation, MIST appears to negatively regulate receptor-induced PLC $\gamma$ 2 activation. Although NK cells lacking both Syk and ZAP-70 apparently still retain NKR-P1C–induced IFN- $\gamma$  production, the function of Syk family PTKs in NKR-P1C–induced IFN- $\gamma$  production appears to be masked by the existence of other synergistic and redundant signaling pathways mediated by Src family PTKs and/or PI3-kinase, because cytotoxic responses of Syk/ZAP-70–double-deficient NK cells are more sensitive to Src kinase and PI3-kinase inhibitors than those of wild-type cells.<sup>37</sup> Furthermore, these 3 NK-cell receptor–proximal signaling pathways appear to converge on PLC $\gamma$ 2, because PLC $\gamma$ 2-deficient NK cells failed to activate both non-ITAM– and ITAM-bearing NK-cell receptor–mediated activation.<sup>31,38</sup> MIST may negatively regulate a broad range of activating NK-cell receptor signaling upstream of or at the level of PLC $\gamma$ 2.

Our analysis of the structure-function relationship of MIST using retrovirus-mediated reconstitution of MIST-deficient NK cells with various MIST mutants indicates that the C-terminal proline-rich region of MIST is required for the negative function of MIST in NKR-P1C–induced IFN- $\gamma$  production by NK cells. Furthermore, ectopic expression of Fgr in MIST-deficient and -sufficient CD4<sup>+</sup>NKT cells that lack endogenous Fgr revealed that the interaction of MIST with Fgr is required for repressing NK-cell receptor–induced IFN- $\gamma$  production. This model was also supported by our observation that the nonfunctional SH3 domain mutant of Fgr, which is unable to associate with MIST, failed to reverse the enhanced NKR-P1C–induced IFN- $\gamma$  production by Fgr-deficient NK cells. One obvious question is how MIST and Fgr collaborate to inhibit the activation of NK-cell receptor signaling. In this regard, it has been reported that Fgr in monocytes inhibits  $\beta$ 2 integrin signaling through a direct association between the Fgr SH2 domain and a phosphorylated tyrosine residue (Tyr342) in the

Syk linker region, which down-regulates Syk activity.<sup>26</sup> This negative regulatory function of Fgr has been postulated to be independent of its kinase activity. We have shown here that the inhibitory function of Fgr in NKR-P1C–induced IFN- $\gamma$  production is mediated by its SH3 domain, a MIST-binding site, but not its kinase domain. We have previously demonstrated that MIST can associate with the SH2 and SH3 domains of PLC $\gamma$  through the phosphorylated tyrosine at position 112 and the N-terminal proline-rich domain.<sup>21</sup> MIST is therefore a candidate for the molecule linking Fgr to inhibitory pathways, and it may suppress the Syk-mediated signaling pathway by recruiting PLC $\gamma$ 2, an essential component downstream of Syk, in the vicinity of Fgr-associated Syk and serves as a scaffold for an inactive signaling complex.

An alternative but not mutually exclusive possibility is that the MIST-Fgr complex recruits and activates c-Cbl, an E3 ubiquitin ligase that is known to ubiquitinate and degrade Src family PTKs, PI3-kinase, and Syk/ZAP-70 PTK.<sup>39</sup> c-Cbl has been demonstrated to associate with and monoubiquitinate Fgr,<sup>40</sup> but this monoubiquitination does not cause Fgr protein degradation. c-Cbl is phosphorylated by the cross-linking of several activating NK-cell receptors including CD16<sup>41</sup> and Ly49D.<sup>42</sup> Thus, this MIST-Fgr–nucleated signaling complex containing c-Cbl and PLC $\gamma$ 2 may suppress all 3 pathways from activating NK-cell receptor signaling probably upstream of PLC $\gamma$ 2 activation. Further investigation is necessary to understand the detailed molecular mechanisms of the inhibitory signaling pathway downstream of activating NK-cell receptors.

Utting et al have recently described the NK-cell phenotype of mice deficient in Clnk.<sup>24</sup> Although this phenotype shares some similarities with the MIST-deficient mice described in the current study, IFN- $\gamma$  production was not enhanced. The reason for this discrepancy remains unclear, but it is possible that certain experimental conditions for analyzing IFN- $\gamma$  production by NK cells may differ. For example, we cultured our NK cells for 24 hours with IL-2 to maintain MIST expression, whereas this was not mentioned in the technique of Utting et al. The reduction of MIST expression in wild-type NK cells and the effect on cell viability in both mutant and wild-type NK cells in the absence of IL-2 could also affect the results. Alternatively, the differences in cultivation time for IL-2–expanded NK cells (5 to 7 days in our study and 7 to 9 days in the report by Utting et al) might influence the requirement for MIST/Clnk in receptor-induced IFN- $\gamma$  production, similar to the observed shift in NKG2D signaling from DAP12 to DAP10 by prolonged IL-2 cultivation.<sup>9,43</sup>

In tumor surveillance, it seems likely that the availability of nonself-antigens that are recognizable for NK-cell receptors and associated inflammatory stimuli, particularly cytokines, is key to determining the timing of a generation of subsequent immune reactions against tumors. In this regard, the sequential expression of MIST, initially in NK cells and subsequently in NKT cells, may be suitable to fine-tune the extent and nature of the development of subsequent acquired immune responses. MIST may limit excessive NK-cell activation at the advanced stage of immune responses where abundant cytokines up-regulate MIST expression in NK and CD4<sup>+</sup>NKT cells. Because MIST is required for the full activation of CD4<sup>+</sup>NKT cells in such an advanced stage of immune responses, activated CD4<sup>+</sup>NKT cells expressing MIST produce high amounts of cytokines including IL-4 and IFN- $\gamma$ , which may ultimately determine the nature of subsequent acquired immune responses involving CD8<sup>+</sup> T cells and Th1 or Th2 CD4<sup>+</sup> effector T cells.



## Acknowledgments

We thank Drs H. Arase, K. Takeda, S. Taki, N. Tohyama-Sorimachi, K. Ogasawara, N. Matsumoto, T. Yagi, W. Reith, T.

Kitamura, T. Mizuno, M. Kubo, L. L. Lanier, and C. L. Willman for providing cell lines, plasmids, and helpful discussions; A. Hara for cell sorting; T. Nakao, T. Hara, and S. Takahashi for yeast 2-hybrid screening and tumor metastasis analysis; P. D. Burrows for critical reading of the manuscript; and T. Tada, the former director of our institute, for continuous encouragement.

## References

- Cerwenka A, Lanier LL. Natural killer cells, viruses and cancer. *Nat Rev Immunol*. 2001;1:41-49.
- Godfrey DI, Hammond KJ, Poulton LD, Smyth MJ, Baxter AG. NKT cells: facts, functions and fallacies. *Immunol Today*. 2000;21:573-583.
- Lanier LL. On guard—activating NK cell receptors. *Nat Immunol*. 2001;2:23-27.
- Lantz O, Bendelac A. An invariant T cell receptor alpha chain is used by a unique subset of major histocompatibility complex class I-specific CD4<sup>+</sup> and CD4<sup>-</sup> T cells in mice and humans. *J Exp Med*. 1994;180:1097-1106.
- Bendelac A, Lantz O, Quimby ME, Yewdell JW, Bunnick JR, Bratkiewicz RR. CD1 recognition by mouse NK1<sup>+</sup> T lymphocytes. *Science*. 1995;268:863-865.
- Smith KM, Wu J, Bakker AB, Phillips JH, Lanier LL. Ly-49D and Ly-49H associate with mouse DAP12 and form activating receptors. *J Immunol*. 1998;161:7-10.
- Arase N, Arase H, Park SY, Ohno H, Ra C, Saito T. Association with FcR $\gamma$  is essential for activation signal through NKR-P1 (CD161) in natural killer (NK) cells and NK1.1<sup>+</sup> T cells. *J Exp Med*. 1997;186:1957-1963.
- Wu J, Song Y, Bakker AB, et al. An activating immunoreceptor complex formed by NKG2D and DAP10. *Science*. 1999;285:730-732.
- Gilfillan S, Ho EL, Cella M, Yokoyama WM, Colonna M. NKG2D recruits two distinct adapters to trigger NK cell activation and costimulation. *Nat Immunol*. 2002;3:1150-1155.
- Jordan MS, Singer AL, Koretzky GA. Adaptors as central mediators of signal transduction in immune cells. *Nat Immunol*. 2003;4:110-116.
- Pivniouk V, Tsitsikov E, Swinton P, Rathbun G, Alt FW, Geha RS. Impaired viability and profound block in thymocyte development in mice lacking the adaptor protein SLP-76. *Cell*. 1998;94:229-238.
- Clements JL, Yang B, Ross-Barta SE, et al. Requirement for the leukocyte-specific adapter protein SLP-76 for normal T cell development. *Science*. 1998;281:416-419.
- Clements JL, Lee JR, Gross B, et al. Fetal hemorrhage and platelet dysfunction in SLP-76-deficient mice. *J Clin Invest*. 1999;103:19-25.
- Pivniouk VI, Martin TR, Lu-Kuo JM, Katz HR, Oettgen HC, Geha RS. SLP-76 deficiency impairs signaling via the high-affinity IgE receptor in mast cells. *J Clin Invest*. 1999;103:1737-1743.
- Jumaa H, Wollscheid B, Mitterer M, Wienands J, Reth M, Nielsen PJ. Abnormal development and function of B lymphocytes in mice deficient for the signaling adaptor protein SLP-65. *Immunity*. 1999;11:547-554.
- Pappu R, Cheng AM, Li B, et al. Requirement for B cell linker protein (BLNK) in B cell development. *Science*. 1999;286:1949-1954.
- Hayashi K, Nittono R, Okamoto N, et al. The B cell-restricted adaptor BASH is required for normal development and antigen receptor-mediated activation of B cells. *Proc Natl Acad Sci U S A*. 2000;97:2755-2760.
- Xu S, Tan JE, Wong EP, Manickam A, Ponniah S, Lam KP. B cell development and activation defects resulting in xid-like immunodeficiency in BLNK/SLP-65-deficient mice. *Int Immunol*. 2000;12:397-404.
- Cao MY, Davidson D, Yu J, Latour S, Veillette A. Clnk, a novel SLP-76-related adaptor molecule expressed in cytokine-stimulated hemopoietic cells. *J Exp Med*. 1999;190:1527-1534.
- Goitsuka R, Kanazashi H, Sasanuma H, et al. A BASH/SLP-76-related adaptor protein MIST/Clnk involved in IgE receptor-mediated mast cell degranulation. *Int Immunol*. 2000;12:573-580.
- Goitsuka R, Tatsuno A, Ishiai M, Kurosaki T, Kitamura D. MIST functions through distinct domains in immunoreceptor signaling in the presence and absence of LAT. *J Biol Chem*. 2001;276:36043-36050.
- Fujii Y, Wakahara S, Nakao T, et al. Targeting of MIST to Src-family kinases via SKAP55-SLAP-130 adaptor complex in mast cells. *FEBS Lett*. 2003;540:111-116.
- Yu J, Riou C, Davidson D, et al. Synergistic regulation of immunoreceptor signaling by SLP-76-related adaptor Clnk and serine/threonine protein kinase HPK-1. *Mol Cell Biol*. 2001;21:6102-6112.
- Utting O, Sedgmen BJ, Watts TH, et al. Immune functions in mice lacking Clnk, an SLP-76-related adaptor expressed in a subset of immune cells. *Mol Cell Biol*. 2004;24:6067-6075.
- Lowell CA, Soriano P, Varmus HE. Functional overlap in the src gene family: inactivation of hck and fgr impairs natural immunity. *Genes Dev*. 1994;8:387-398.
- Vines CM, Potter JW, Xu Y, et al. Inhibition of  $\beta$ 2 integrin receptor and Syk kinase signaling in monocytes by the Src family kinase Fgr. *Immunity*. 2001;15:507-519.
- Nosaka T, Kawashima T, Misawa K, Ikuta K, Mui AL, Kitamura T. STAT5 as a molecular regulator of proliferation, differentiation and apoptosis in hematopoietic cells. *EMBO J*. 1999;18:4754-4765.
- Baker BW, Boettiger D, Spooner E, Norton JD. Efficient retroviral-mediated gene transfer into human B lymphoblastoid cells expressing mouse ecotropic viral receptor. *Nucleic Acids Res*. 1992;20:5234.
- Kawano T, Cui J, Koezuka Y, et al. CD1d-restricted and TCR-mediated activation of  $\alpha$  $\nu$ 14 NKT cells by glycosylceramides. *Science*. 1997;278:1626-1629.
- Chuang SS, Kumaresan PR, Mathew PA. 2B4 (CD244)-mediated activation of cytotoxicity and IFN- $\gamma$  release in human NK cells involves distinct pathways. *J Immunol*. 2001;167:6210-6216.
- Tassi I, Presti R, Kim S, Yokoyama WM, Gilfillan S, Colonna M. Phospholipase C- $\gamma$ 2 is a critical signaling mediator for murine NK cell activating receptors. *J Immunol*. 2005;175:749-754.
- Chiodoni C, Stoppacciaro A, Sangaletti S, et al. Different requirements for  $\alpha$ -galactosylceramide and recombinant IL-12 antitumor activity in the treatment of C-26 colon carcinoma hepatic metastases. *Eur J Immunol*. 2001;31:3101-3110.
- Hayakawa Y, Takeda K, Yagita H, et al. Critical contribution of IFN- $\gamma$  and NK cells, but not perforin-mediated cytotoxicity, to anti-metastatic effect of  $\alpha$ -galactosylceramide. *Eur J Immunol*. 2001;31:1720-1727.
- Colucci F, Di Santo JP, Leibson PJ. Natural killer cell activation in mice and men: different triggers for similar weapons? *Nat Immunol*. 2002;3:807-813.
- Negishi I, Motoyama N, Nakayama K, et al. Essential role for ZAP-70 in both positive and negative selection of thymocytes. *Nature*. 1995;376:435-438.
- Cheng AM, Rowley B, Pao W, Hayday A, Bolen JB, Pawson T. Syk tyrosine kinase required for mouse viability and B-cell development. *Nature*. 1995;378:303-306.
- Colucci F, Schweighoffer E, Tomasello E, et al. Natural cytotoxicity uncoupled from the Syk and ZAP-70 intracellular kinases. *Nat Immunol*. 2002;3:288-294.
- Wang D, Feng J, Wen R, et al. Phospholipase C $\gamma$ 2 is essential in the functions of B cell and several Fc receptors. *Immunity*. 2000;13:25-35.
- Duan L, Reddi AL, Ghosh A, Dimri M, Band H. The Cbl family and other ubiquitin ligases: destructive forces in control of antigen receptor signaling. *Immunity*. 2004;21:7-17.
- Melander F, Andersson T, Dib K. Fgr but not Syk tyrosine kinase is a target for  $\beta$ 2 integrin-induced c-Cbl-mediated ubiquitination in adherent human neutrophils. *Biochem J*. 2003;370:687-694.
- Cerboni C, Gismondi A, Palmieri G, et al. CD16-mediated activation of phosphatidylinositol-3 kinase (PI-3K) in human NK cells involves tyrosine phosphorylation of Cbl and its association with Grb2, Shc, pp36 and p85 PI-3K subunit. *Eur J Immunol*. 1998;28:1005-1015.
- McVicar DW, Taylor LS, Gosselin P, et al. DAP12-mediated signal transduction in natural killer cells: a dominant role for the Syk protein-tyrosine kinase. *J Biol Chem*. 1998;273:32934-32942.
- Diefenbach A, Tomasello E, Lucas M, et al. Selective associations with signaling proteins determine stimulatory versus costimulatory activity of NKG2D. *Nat Immunol*. 2002;3:1142-1149.